



Synthesis and PhotoLuminescent Characteristics of Eu^{2+} -Activated Dicalcium magnesiumdisilicate Blue-Emitting Phosphors for High Power White LEDs

Dipti Shukla , Ambuj Pandey

O.P Jindal University, Raigarh , (C.G) India

Abstract: The phosphors $\text{Ca}_2\text{MgSi}_2\text{O}_7:\text{Eu}^{2+}$ have been successfully prepared by high temperature solid-state reaction process. . This used synthesis method is simple, time saving, and cost effective. X-ray power diffraction (XRD) analysis for characterize the crystallography structure, and SEM images were recorded for determine the topography, morphology, composition. Photoluminescence emission (PL) and excitation (PLE) measurements were investigated. Under the ultra violet excitation of 315 nm, the emission spectrum shows a strong band with a peak at about 462 nm. The results represented the type of phosphor may have potential applications in the fields of Ultra-Violet (UV) excited white LEDs.

Keywords: XRD, SEM, PHOTOLUMINESCENCE (PL)

Introduction: A phosphor is a substance which light.” A phosphor includes both phosphorescent material and fluorescent material. The phosphorescent materials show slow decay ($\geq 1\text{ms}$) in brightness and these materials are used in radar screen ,whereas fluorescent materials in which emission decay takes place over tens of nanosecond and these materials are used in cathode ray tube (CRT) display and plasma video display screen and white LED . So that phosphors are manufactured in ways to make them most suitable for consistent, high yield LED manufacturing. LED chips are intrinsically green, blue or red with the blue variety of LEDs are the most commonly used in solid state lighting (SSL). It is well known that silicate host was attracting more attention in the application of long afterglow phosphor (Bo Liu *et al.*, 2005). So due to these characteristics, silicate phosphors plays a important role in LED. White-light-emitting diodes (w-LEDs) attract more interest as the result of their advantages like longer lifetime, higher rendering index, higher luminosity efficiency, and lower energy consumption [1, 2]. Divalent europium (Eu^{2+}) doped commercially blue phosphors are used in plasma display tube. Eu^{2+} ions play a significant role in the rare earth ions; commonly, they act as the blue-emitting phosphors due to the parity allowed electric dipole transition of $4f \rightarrow 5d$. Eu^{2+} -activated phosphors commonly act as the blue-emitting phosphors as the result of their $4f^1$ configuration in solids shows efficient broad band luminescence which due to the parity allowed electric dipole transition.

In this paper, we investigate the advantages of $\text{Ca}_2\text{MgSi}_2\text{O}_7$ as the substrate of luminescent material and doped divalent rare earth Eu^{2+} to analyze the luminescence properties under ultraviolet excitation conditions. $\text{Ca}_2\text{MgSi}_2\text{O}_7:\text{Eu}^{2+}$ phosphors was prepared by the solid-state reaction; corresponding photo-luminescent properties were investigated in detail; the CIE of phosphors were also calculated. The results suggest that $\text{Ca}_2\text{MgSi}_2\text{O}_7:\text{Eu}^{2+}$ may be used as potential blue phosphors for UV-based w-LEDs.

Experimental Section

2.1. Synthesis of $\text{Ca}_2\text{MgSi}_2\text{O}_7:\text{Eu}^{2+}$ ~ Phosphors

The phosphor sample was prepared by solid state diffusion reaction method. The phosphor $\text{Ca}_2\text{MgSi}_2\text{O}_7$ is prepared from the compounds calcium carbonate (CaCO_3) and magnesium oxide (MgO), SiO_2 and Eu_2O_3 . The prepared phosphor $\text{Ca}_2\text{MgSi}_2\text{O}_7$ is weighed and grounded into a fine powder using agate mortar and pestle about an hour. The grounded mixture was placed in an alumina crucible and heated from room temperature to 1200°C in a muffle furnace with a heating rate of $5^\circ\text{C}/\text{min}$. After reaching 1200°C the phosphor heated for 3 hours and the furnace was allowed to cool to room temperature along with the samples.

2.2. Characterization of $\text{Ca}_2\text{MgSi}_2\text{O}_7:\text{Eu}^{2+}$ ~ Phosphors

The X ray diffractometer used in this study is Bruker AXS diffractometer with $\text{Cu K}\alpha$ radiation (\AA); the operation voltage and current were maintained at 40 kV and 40 mA, respectively; a scan rate of $2^\circ/\text{min}$ was applied to record the patterns in the range of $2\theta = 10\sim 60$. Photoluminescence was recorded by RF-5301 PC SHIMADZU Spectrofluorophotometer (RF 5301 PC). Emission and excitation were recorded using a 1.5 nm width of spectral slit. Photoluminescence measurement is a simple non-destructive and versatile technique.

3. Result and Discussion

3.1. The Crystal Structures of the $\text{Ca}_2\text{MgSi}_2\text{O}_7:\text{Eu}^{2+}$ ~ Phosphors

The phase and structure of the prepared samples were checked by using XRD spectra. All samples showed which can be indexed to $\text{Ca}_2\text{MgSi}_2\text{O}_7$ in a tetragonal structure (JCPDS 35-592). This single phase sample is well crystallized at 1200°C for 3 hour. From the figures 1, 2 it can be seen that the major peak of $\text{Ca}_2\text{MgSi}_2\text{O}_7$ at $2\theta = 31.24^\circ$ and the main peak of rare earth Eu doped akermanite $\text{Ca}_2\text{MgSi}_2\text{O}_7$ at 31.20° respectively. Since no impurity phase was observed in any of the samples. It clearly implies that the obtained samples are single phase and doping does not cause any significant change in the host structure or lattice distortions. The crystalline sizes (D) and strain of various samples are estimated using Scherrer's formula and FWHM method. According to which $D = K\lambda / \beta \cos \theta$ and strain $\epsilon = \lambda / \sin \theta [\beta \cos \theta / \lambda - K/D]$ where K is the Scherrer's constant, λ -the X-ray wavelength of $\text{Cu-K}\alpha$ radiations (1.54\AA), β -the peak width of half-maximum (FWHM) and θ is the Bragg's diffraction angle. The calculated average crystallite size is about 67 nm. The corresponding XRD data for indexed are summarized in table 1. The strain ϵ is estimated from the slope of the line and the crystalline size.

Table 1: XRD Crystal data of $\text{Ca}_2\text{MgSi}_2\text{O}_7:\text{Eu}^{2+}$ ~ Phosphors

Composition	Size by crystalline	Band Gap	Strain
$\text{Ca}_2\text{MgSi}_2\text{O}_7$	19.69	5.2	0.22 ^o
$\text{Ca}_2\text{MgSi}_2\text{O}_7:\text{Eu}^{2+}$	19.62 ^o	5.2	0.21 ^o

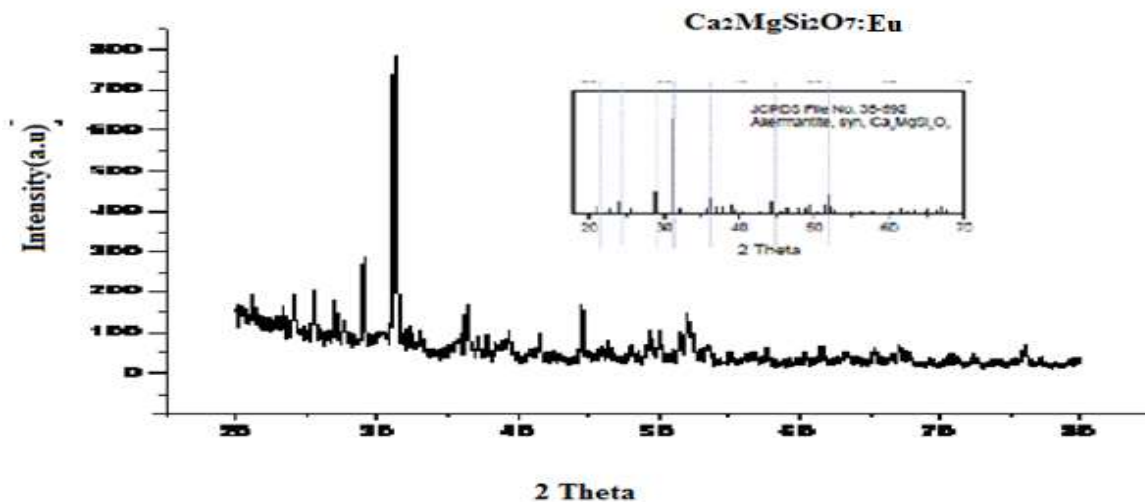


Fig: Typical XRD Pattern of Eu doped akermanite $\text{Ca}_2\text{MgSi}_2\text{O}_7$

3.2 Surface Morphology (SEM) of $\text{Ca}_2\text{MgSi}_2\text{O}_7:\text{Eu}^{2+}$ ~ Phosphors

Fig shows the SEM images of rare earth Eu^{2+} doped prepared sample. The surface part of prepared samples at high magnification are spherical, smooth and homogeneous but isolated aggregate but in case of low magnification the micrograph show that the particles are micro size, irregular shape and aggregated.

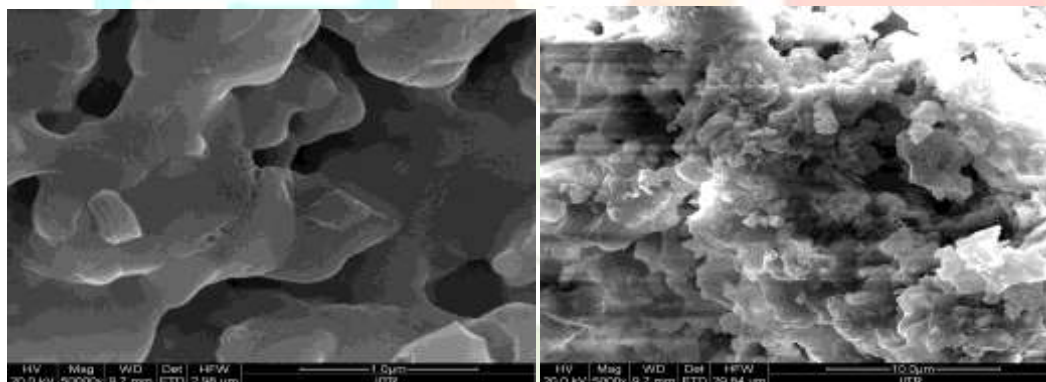


Fig: SEM morphology of Eu^{2+} doped $\text{Ca}_2\text{MgSi}_2\text{O}_7$ phosphor (a) at high magnification (b) at low magnification

3.3. The PL Excitation and Emission Spectra of Eu^{2+} doped $\text{Ca}_2\text{MgSi}_2\text{O}_7$ phosphor

Fig I(a) and fig I(b) shows the PL spectra of $\text{Ca}_2\text{MgSi}_2\text{O}_7:\text{Eu}^{2+}$ when excited 462nm. The excitation spectrum was observed in the range of 220–400 nm and emission spectra were recorded in the range of 400–650 nm. The excitation broad band due to transitions of $^8\text{S}_{7/2} (4f^7)$ ground state to the higher energy state (excited state) $4f^65d^1$ [$^8\text{S}_{7/2} (4f^7) \rightarrow 4f^65d^1$] configuration were observed under the ultra violet excitation. The excitation spectrum of the blue fluorescence ($\lambda_{em} = 462 \text{ nm}$) shows two broad band's with their peaks at about 267 and 315 nm, respectively, which are due to the crystal field splitting of the Eu^{2+} d orbital. Under the ultra violet excitation of 315 nm, the emission spectrum shows a strong band with a peak at about 462 nm for all concentration of Eu^{2+} ,

which corresponds to $4f \rightarrow 5d$ transition of Eu^{2+} ions. In Eu^{2+} ion, the 5d energy level and the lower level of 4f state is overlap, so that the electron of 4f state can be excited to 5d state. The broad luminescence of Eu^{2+} is due to $4f^6 5d^1 \rightarrow 4f^7$ transitions. It is known that the blue emission peaked at 462 nm corresponds to the PL emission spectra of samples were recorded for the excitation wavelength of 462 nm. The excitation of the $\text{Ca}_2\text{MgSi}_2\text{O}_7:\text{Eu}^{2+}$ phosphor with 462 nm wavelength generates photoluminescence emission at 237, 252 and 267 nm, 315 nm with intensities of around 550 a.u. transitions of ${}^4\text{F}_{9/2} \rightarrow {}^6\text{H}_{15/2}$ and this emission belongs to hypersensitive transition with $J = 2$. The prepared $\text{Ca}_2\text{MgSi}_2\text{O}_7:\text{Eu}^{2+}$ phosphor would emit blue light with peak at 462 nm [9, 10].

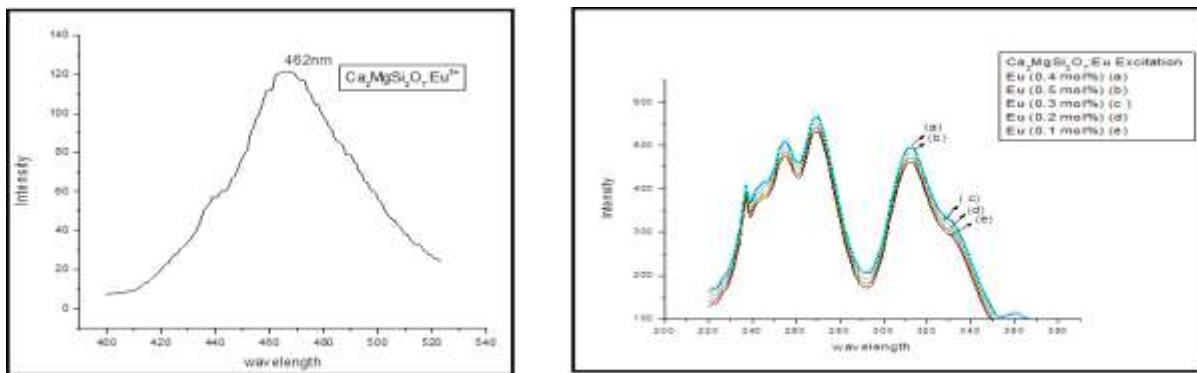


Fig: Emission and Excitation Spectra of Eu^{2+} doped $\text{Ca}_2\text{MgSi}_2\text{O}_7$ phosphor.

3.4 Emission spectra of Eu^{2+} doped $\text{Ca}_2\text{MgSi}_2\text{O}_7$ phosphor with different concentration of dopant

It can be also observed that the emission spectra for rare earth ions Eu^{2+} doped $\text{Ca}_2\text{MgSi}_2\text{O}_7$ phosphors with different concentration x of 0.01 mol, 0.02 mol, 0.03 mol, 0.04 mol and 0.05 mol respectively. It is well known that lower activator concentration lead to weak luminescence while higher concentration cause concentration quenching. The intensity of the emission increased proportionally with rare earth ions Eu^{2+} concentration until saturation was reached at $x = 0.04$ mol.

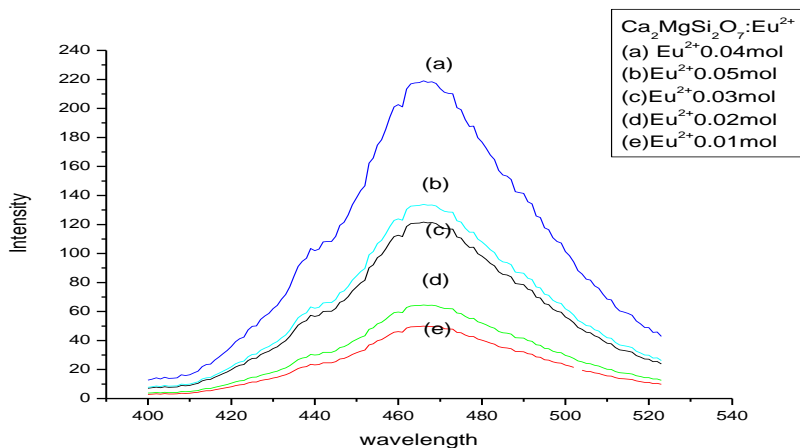
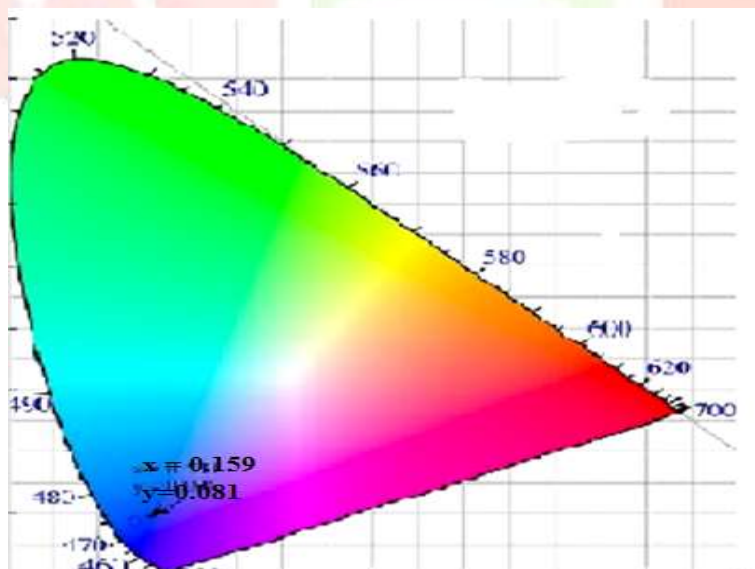


Fig: Emission spectra of Eu²⁺ doped Ca₂MgSi₂O₇ phosphor with different concentration of dopant.

3.5 Chromaticity coordinates (CIE) of Ca₂MgSi₂O₇:Eu²⁺ ~ Phosphor

Figure showed the chromaticity coordinates of optimum molar (0.04 mol) of Eu²⁺-activated Ca₂MgSi₂O₇ phosphors. Based on the standard CIE coordinate color graph, it can be observed that, luminescence colors of Ca₂MgSi₂O₇:Eu²⁺ is placed in (0.159, 0.081) and the color moved to the blue region. When the intensity of Eu²⁺ reaches the maximum, it is more close to the standard CIE of blue light (0.140, 0.080.) it is clearly seen that we have realized that the blue light emission could be excited by UV in Ca₂MgSi₂O₇:Eu²⁺ phosphors, which may be promising for white LEDs under UV excitation.



Conclusions

In summary, a series of $\text{Ca}_2\text{MgSi}_2\text{O}_7:\text{Eu}^{2+}$ phosphors have been synthesized by solid-state reaction. For the PL spectra of Eu^{2+} doped sample it has been observed that, two broad bands with their peaks around at 267nm & 315nm respectively and $\text{Ca}_2\text{MgSi}_2\text{O}_7:\text{Eu}^{2+}$ prepared sample would emits blue light with peak at 462nm. PL spectra at different doping concentrations of Eu^{2+} show optimum emission intensity at $x = 0.04$, after which concentration quenching is observed. When the concentration of Eu^{2+} is 0.4% mol, the chromaticity coordinates of $\text{Ca}_2\text{MgSi}_2\text{O}_7:0.004\text{Eu}^{2+}$ are (0.159, 0.081) which are more close to the standard CIE of blue light (0.140, 0.080). So we can study that $\text{Ca}_2\text{MgSi}_2\text{O}_7:\text{Eu}^{2+}$ phosphors may perform as a blue component for white LEDs.

References

1. C.-H. Huang, Y.-C. Chiu, Y.-T. Yeh, T.-S. Chan, and T.-M. Chen, "Eu²⁺-activated Sr₈ZnSc(PO₄)₇: a novel near-ultraviolet converting yellow-emitting phosphor for white light-emitting diodes," *ACS Applied Materials and Interfaces*, vol. 4, no. 12, pp. 6661–6668, 2012. View at: [Publisher Site](#) | [Google Scholar](#)
2. H. Yu, J. L. Chen, Y. Pu, T. J. Zhang, and S. C. Gan, "Photoluminescence properties of Tb³⁺ and Ce³⁺ co-doped Sr₂MgSi₂O₇ phosphors for solid-state lighting," *Journal of Rare Earths*, vol. 33, no. 4, pp. 366–370, 2015. View at: [Publisher Site](#) | [Google Scholar](#)
3. T. Hussain, L. B. Zhong, M. Danesh et al., "Enabling low amounts of YAG:Ce³⁺ convert blue into white light with plasmonic Au nanoparticles," *Nanoscale*, vol. 7, no. 23, pp. 10350–10356, 2015. View at: [Publisher Site](#) | [Google Scholar](#)
4. Y. Shi, G. Zhu, M. Mikami, Y. Shimomura, and Y. Wang, "A novel Ce³⁺ activated Lu₃MgAl₃SiO₁₂ garnet phosphor for blue chip light-emitting diodes with excellent performance," *Dalton Transactions*, vol. 44, no. 4, pp. 1775–1781, 2015. View at: [Publisher Site](#) | [Google Scholar](#)
5. H. Yu, W. W. Zi, S. Lan et al., "Photoluminescence properties and energy transfer in Ce³⁺/Dy³⁺ co-doped Sr₃MgSi₂O₈ phosphors for potential application in ultraviolet white light-emitting diodes," *Luminescence*, vol. 28, no. 6, pp. 679–684, 2013. View at: [Publisher Site](#) | [Google Scholar](#)
6. F. Baur, F. Glocker, and T. Jüstel, "Photoluminescence and energy transfer rates and efficiencies in Eu³⁺ activated Tb₂Mo₃O₁₂," *Journal of Materials Chemistry C*, vol. 3, no. 9, pp. 2054–2064, 2015. View at: [Publisher Site](#) | [Google Scholar](#)
7. S. Schmiechen, M. Siegert, A. Tücks, P. J. Schmidt, P. Strobel, and W. Schnick, "Narrow-band green emitting nitridolithoalumosilicate Ba[Li₂(Al₂Si₂)N₆]:Eu²⁺ with framework topology whj for LED/LCD-backlighting applications philipp strobel," *Chemistry of Materials*, vol. 27, no. 17, pp. 6109–6115, 2015. View at: [Publisher Site](#) | [Google Scholar](#)
8. A. J. Fernández-Carrión, M. Ocaña, J. García-Sevillano, E. Cantelar, and A. I. Becerro, "New single-phase, white-light-emitting phosphors based on δ-Gd₂Si₂O₇ for solid-state lighting," *The Journal of Physical Chemistry C*, vol. 118, no. 31, pp. 18035–18043, 2014. View at: [Publisher Site](#) | [Google Scholar](#)
9. J. M. Ogiegłó, A. Katelnikovas, A. Zych, T. Jüstel, A. Meijerink, and C. R. Ronda, "Luminescence and luminescence quenching in Gd₃(Ga,Al)₅O₁₂ scintillators doped with Ce³⁺," *Journal of Physical Chemistry A*, vol. 117, no. 12, pp. 2479–2484, 2013. View at: [Publisher Site](#) | [Google Scholar](#)
10. B. Chen, X. S. Qiao, D. F. Peng, and X. P. Fan, "Enhanced luminescence of NaY_{0.6-x}Ce_{0.1}Gd_{0.3}Eu_xF₄ nanorods by energy transfer," *Journal of Applied Physics*, vol. 115, no. 1, pp. 013101–013101, 2014. View at: [Publisher Site](#) | [Google Scholar](#)